

Oxidative Addition of H–SiR₃ to Di- and Triruthenium Carbonyl Complexes Bearing a Bridging Azulene Ligand: Isolation of New Silylruthenium Complexes and Catalytic Hydrosilylation of Ketones

Kouki Matsubara,^{†,§} Kazuhiro Ryu,[‡] Tomoyuki Maki,[‡] Takafumi Iura,[‡] and Hideo Nagashima^{*,†,‡,§}

Institute of Advanced Material Study, Interdisciplinary Graduate School of Engineering Sciences, and CREST, Japan Science and Technology Corporation (JST), Kyushu University, Kasuga, Fukuoka 816-8580, Japan

Received January 2, 2002

Oxidative addition of PhMe₂SiH to di- and triruthenium carbonyl clusters bearing 4,6,8-trimethylazulene as the bridging ligand was studied in relation to mechanisms of hydrosilylation of ketones catalyzed by these complexes. Reaction of PhMe₂SiH with (μ₃,η⁵:η⁵-4,6,8-trimethylazulene)Ru₃(CO)₇ (**3**) resulted in liberation of a CO ligand, oxidative addition of the Si–H bond, and hydrogenation of one carbon–carbon double bond in the azulene ligand to form a novel 46-electron cluster, (μ₂,η³:η⁵-4,5-dihydro-4,6,8-trimethylazulene)Ru₃(H)(SiMe₂Ph)(CO)₆ (**6**). In contrast, (μ₂,η³:η⁵-4,6,8-trimethylazulene)Ru₂(CO)₅ (**4**) reacted with HMe₂SiPh to give (μ₂,η³:η⁵-4,5-dihydro-4,6,8-trimethylazulene)Ru₂(CO)₅(SiMe₂Ph)₂ (**7**), which has a unique Ru→Ru dative bond, by way of oxidative addition of two molecules of PhMe₂SiH to the starting diruthenium complex followed by hydrogenation of a carbon–carbon double bond in the azulene ligand. In contrast to the fact that the diruthenium complexes **4** and **7** are not catalytically active, the triruthenium clusters **3** and **6** are catalysts for the hydrosilylation of acetophenone with moderate catalytic activity. NMR observation of intermediates in the catalytic hydrosilylation of acetophenone using **6** as catalyst suggests the existence of a reaction pathway without a cluster fragmentation, in which the triruthenium cluster is involved in the catalytic cycle.

Introduction

Transition metal catalyzed hydrosilylation of unsaturated molecules is one of the powerful tools in the synthesis of organosilicon compounds, which themselves are useful for the production of silicon-based organic materials and polymers and for unique intermediates in organic synthesis.¹ A number of transition metal salts or complexes are known to be active toward catalytic hydrosilylation. In particular, numerous experimental as well as theoretical studies have been undertaken using mononuclear rhodium or platinum compounds.²

In contrast, reactions involving activation of hydrosilanes by multinuclear metal carbonyls have not been investigated fully. In the cluster-catalyzed hydrosilylation, multinuclear intermediates may be involved in the catalytic cycle. This may lead to reactivities and selectivities different from those accomplished by conventional rhodium-phosphine- or platinum-based catalysts.³ In fact, Co₂(CO)₈ catalyzes both hydrosilylation and silylformylation of unsaturated molecules,⁴ and catalytic cycles that include silyl-cobalt intermediates have been proposed.⁵ Studies by Matsuda and Ojima on tetranuclear Rh or Co–Rh mixed carbonyls revealed their high reactivity in the silylformylation of alkynes and in other reactions.^{6,7} Mechanisms involving possible intermediates with various nuclearity have been discussed on the basis of the analysis of metallic species

[†] Institute of Advanced Material Study.

[‡] Interdisciplinary Graduate School of Engineering Sciences.

[§] CREST.

(1) For reviews for catalytic hydrosilylation reactions: (a) *Comprehensive Handbook on Hydrosilylation*; Marciniec, B. Ed.; Pergamon Press: Oxford, 1992. (b) Marciniec, B. In *Applied Homogeneous Catalysis with Organometallic Compounds*; Cornils, B., Herrmann, W. A., Eds.; VCH: Weinheim, 1996; Vol. 1, Chapter 2.6, p 487. (c) Ojima, I. In *The Chemistry of Organosilicon Compounds*; Patai, S., Rappoport, Z., Eds.; Wiley: New York, 1989; p 1479. (d) Brook, M. A. In *Silicon in Organic, Organometallic, and Polymer Chemistry*; Wiley: New York, 2000; Chapter 12.8, p 401. (e) Spier, J. L. *Adv. Organomet. Chem.* **1978**, *17*, 407.

(2) (a) Chalk, A. J.; Harrod, J. F. *J. Am. Chem. Soc.* **1967**, *89*, 1640. (b) A recent experimental work on the mechanisms of catalytic hydrosilylation: Maruyama, Y.; Yamamura, K.; Nakayama, I.; Yoshitani, K.; Ozawa, F. *J. Am. Chem. Soc.* **1998**, *120*, 1421, and references therein. (c) A recent representative report for theoretical studies on the mechanisms of hydrosilylation: Sakaki, S.; Mizoe, N.; Sugimoto, M.; Musashi, Y. *Coord. Chem. Rev.* **1999**, *190–192*, 933, and references therein.

(3) For recent general reviews on organometallic clusters: (a) *Catalysis by Di- and Polynuclear Metal Cluster Complexes*; Adams, R. D., Cotton, F. A., Eds.; Wiley-VCH: Canada, 1998. (b) *Metal Clusters in Chemistry*; Braunstein, P., Oro, L. A., Raithby, P. R., Eds.; Wiley-VCH: Weinheim, 1999. (c) González-Moraga, G. *Cluster Chemistry*; Springer-Verlag: Berlin, 1993. (d) *The Chemistry of Metal Cluster Complexes*; Shriver, D. F., Kaesz, H. D., Adams, R. D., Eds.; VCH Publishers: New York, 1990. (e) Braunstein, P. *Perspect. Coord. Chem.* **1992**, *67*. (f) Süß-Fink, G.; Meister, G. *Adv. Organomet. Chem.* **1993**, *35*, 41.

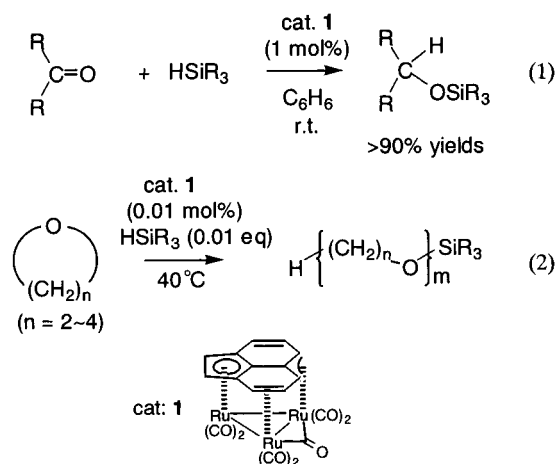
(4) Murai, S.; Sonoda, N. *Angew. Chem., Int. Ed. Engl.* **1979**, *18*, 837.

(5) (a) Seitz, F.; Wrighton, M. S. *Angew. Chem., Int. Ed. Engl.* **1988**, *27*, 289. (b) Sakurai, H.; Miyoshi, K.; Nakadaira, Y. *Tetrahedron Lett.* **1977**, 2671. (c) Chatani, N.; Komada, T.; Kajiwara, Y.; Murakami, H.; Kakiuchi, F.; Ikeda, S.; Murai, S. *Chem. Lett.* **2000**, 14.

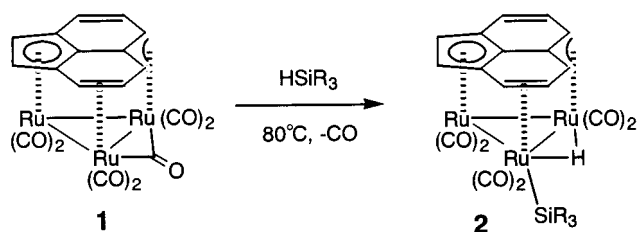
formed in the reactions of the clusters with either unsaturated substrates or organosilanes.⁷ However, it has been difficult to specify the net active species, because the reactions often involve cluster fragmentation.^{7c-e}

Although not very many examples have been reported on the ruthenium carbonyl catalyzed hydrosilylation,⁸ reactions of hydrosilanes with several ruthenium carbonyl clusters have been investigated.⁹⁻¹² Products of the reactions of Ru₃(CO)₁₂ with hydrosilanes were found to be dependent on the structure of silanes used, and in many cases, cluster fragmentation was involved.^{8,9} Certain ruthenium clusters, (μ_3 -6-methylaminopyridine)-Ru₃(μ -H)(CO)₉,^{10a-d} [(μ_2 -3,5-dimethylpyrazole)Ru₃(μ -H)(μ -CO)₃(CO)₇]⁻,^{10e} and [Ru₃(μ -H)(μ -NO)(CO)₁₀]⁻,^{10f} the trimetallic framework of which is reinforced by the introduction of bridging ligands, undergo oxidative addition of hydrosilanes without cluster fragmentation to form the corresponding triruthenium clusters with Ru-Si bonds. Little is known about catalytic hydrosilylations using these clusters. An important report from the viewpoint of both reactions and mechanisms was published by G. Süss-Fink, in which [Ru₃H(CO)₁₁]⁻ was reversibly reacted with two molecules of HSiR₃ to form [Ru₃H(SiR₃)₂(CO)₁₀]⁻ and where both of the clusters exhibited catalytic activity toward silylformylation and hydrosilylation of ethylene at 100 °C.¹¹ However, the characterization of the clusters and the characteristics of the catalytic reactions have not been reported in detail. Thus, all of these data in the literature suggest that further investigation is warranted in order to figure out whether cluster intermediates are involved in the hydrosilylation reactions catalyzed by organometallic clusters.

Scheme 1



Scheme 2



Previously we reported that a triruthenium carbonyl cluster bearing a μ_3 -acenaphthylene ligand, ($\mu_3, \eta^2: \eta^3: \eta^5$ -acenaphthylene)Ru₃(CO)₇ (**1**), is an active catalyst for the hydrosilylation of ketones and aldehydes (Scheme 1, eq 1), the reduction of acetals and cyclic ethers, and the ring-opening polymerization of cyclic ethers (Scheme 1, eq 2).¹² The silyl-ruthenium cluster, ($\mu_3, \eta^2: \eta^3: \eta^5$ -acenaphthylene)Ru₃(H)(SiR₃)(CO)₆ (**2**), was isolated from the reaction of **1** with R₃SiH, which is a possible intermediate in the catalytic cycle, contributing to activating the Si-H bond in hydrosilanes for the reaction with organic molecules (Scheme 2). However, it was proven experimentally that **2** is not active toward hydrosilylation of ketones. Although NMR studies to detect the net catalytic species revealed that unstable species with a structure similar to **2** exist in the reaction solution of **1** and PhMe₂SiH, further characterization of this species was hampered because of its instability.¹² Within this context, we were interested in the catalytic and stoichiometric reactions of ($\mu_3, \eta^2: \eta^3: \eta^5$ -4,6,8-trimethylazulene)Ru₃(CO)₇ (**3**) with R₃SiH.¹³ Since **3** has a structure closely related to **1**, a similar reaction behavior was anticipated in the reaction with R₃SiH. A further advantage in the investigation of **3** is that analogous compounds with a different nuclearity, as shown in Figure 1, ($\mu_2, \eta^3: \eta^5$ -4,6,8-trimethylazulene)Ru₂(CO)₅ (**4**) and ($\mu_3, \eta^5: \eta^5$ -4,6,8-trimethylazulene)Ru₄(CO)₉ (**5**), could also be subjected to stoichiometric and catalytic reactions with hydrosilanes, which should provide further elucidation of the effect of nuclearity on the reactivity of ruthenium carbonyl clusters toward R₃SiH.¹³

In this paper, we wish to report the difference in catalytic activity among **1**, **3**, **4**, and **5** using the

(6) (a) Matsuda, I.; Ogiso, A.; Sato, S.; Izumi, Y. *J. Am. Chem. Soc.* **1989**, *111*, 2332. (b) Ojima, I.; Donovan, R. J.; Clos, N. *Organometallics* **1991**, *10*, 2606.

(7) (a) Matsuda, I.; Fukuta, Y.; Tsuchihashi, T.; Nagashima, H.; Itoh, K. *Organometallics* **1997**, *16*, 4327. (b) Ojima, I.; Clos, N.; Donovan, R. J.; Ingallina, P. *Organometallics* **1990**, *9*, 3127. (c) Ojima, I.; Ingallina, P.; Donovan, R. J.; Clos, N. *Organometallics* **1991**, *10*, 38. (d) Ojima, I.; Donovan, R. J.; Ingallina, P.; Clos, N.; Shay, W. R.; Eguchi, M.; Zeng, Q.; Korda, A. *J. Cluster Sci.* **1992**, *3*, 423. (e) Ojima, I.; Li, Z.; Donovan, R. J.; Ingallina, P. *Inorg. Chim. Acta* **1998**, *270*, 279.

(8) (a) Nesmeyanov, A. N.; Friedlina, R. K.; Chuskovskaya, E. C.; Petrov, R. G.; Belyavsky, A. B. *Tetrahedron* **1962**, *17*, 61. (b) Ojima, I.; Fuchikami, T.; Yatabe, M. *J. Organomet. Chem.* **1981**, *221*, C36. (c) Seki, Y.; Takeshita, K.; Kawamoto, K.; Murai, S.; Sonoda, N. *J. Org. Chem.* **1986**, *51*, 3890. (d) Seki, Y.; Takeshita, K.; Kawamoto, K.; Murai, S.; Sonoda, N. *Angew. Chem., Int. Ed. Engl.* **1980**, *19*, 928. (e) Hilal, H. S.; Khalaf, S.; Jondi, W. *J. Organomet. Chem.* **1993**, *452*, 167.

(9) (a) Buuren, G. N.; Willis, A. C.; Einstein, W. B.; Peterson, R. K.; Pomeroy, R. K.; Sutton, D. *Inorg. Chem.* **1981**, *20*, 4361. (b) Brookes, A.; Knox, S. A. R.; Stone, F. G. A. *J. Chem. Soc. (A)* **1971**, 3469. (c) Knox, S. A. R.; Stone, F. G. A. *J. Chem. Soc. (A)* **1969**, 2559. (d) Vancea, L.; Graham, W. A. G. *Inorg. Chem.* **1974**, *13*, 511. (e) Kotani, S.; Tanizawa, T.; Adachi, T.; Yoshida, T.; Sonogashira, K. *Chem. Lett.* **1994**, 1665. (f) Braunstein, P.; Galsworthy, J. R.; Massa, W. *J. Chem. Soc., Dalton Trans.* **1997**, 4677.

(10) (a) Cabeza, J. A.; Fernandez-Colinas, J. M.; Garcia-Granda, S.; Llamazares, A.; Lopez-Ortiz, F.; Riera, V.; Van der Maelen, J. F. *Organometallics* **1994**, *13*, 426. (b) Cabeza, J. A.; Garcia-Granda, S.; Llamazares, A.; Riera, V.; Van der Maelen, J. F. *Organometallics* **1993**, *12*, 2973. (c) Cabeza, J. A.; Llamazares, A.; Riera, V.; Triki, S.; Ouahab, L. *Organometallics* **1992**, *11*, 3334. (d) Cabeza, J. A.; Franco, R. J.; Llamazares, A.; Riera, V.; Bois, C.; Jeannin, Y. *Inorg. Chem.* **1993**, *32*, 4640. (e) Cabeza, J. A.; Franco, R. J.; Riera, V.; Garcia-Granda, S.; Van der Maelen, J. F. *Organometallics* **1995**, *14*, 3342. (f) Cabeza, J. A.; Franco, R. J.; Riera, V. *Inorg. Chem.* **1994**, *33*, 5952.

(11) (a) Süss-Fink, G.; Ott, J.; Schmidkonz, B.; Guldner, K. *Chem. Ber.* **1982**, *115*, 2487. (b) Süss-Fink, G.; Reiner, J. *J. Mol. Catal.* **1982**, *16*, 231. (c) Süss-Fink, G. *Angew. Chem., Int. Ed. Engl.* **1982**, *21*, 73. (d) Süss-Fink, G.; Reiner, J. *J. Organomet. Chem.* **1981**, *221*, C36.

(12) Nagashima, H.; Suzuki, A.; Iura, T.; Ryu, K.; Matsubara, K. *Organometallics* **2000**, *19*, 3579.

(13) Nagashima, H.; Suzuki, A.; Nobata, M.; Aoki, K.; Itoh, K. *Bull. Chem. Soc. Jpn.* **1998**, *71*, 2441.

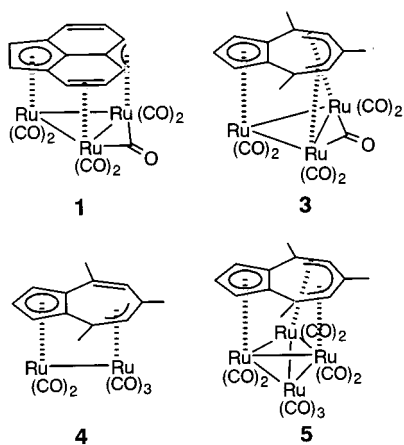


Figure 1. Multinuclear ruthenium compounds with bridging conjugate π -electron ligands, **1**, **3**, **4**, and **5**.

hydrosilylation of acetophenone with PhMe_2SiH as a probe. The products obtained from the reaction of PhMe_2SiH with **3** or **4**, which show a moderate or low catalytic activity toward hydrosilylation, were characterized as possible intermediates in the catalytic cycle. It is important that the reaction of PhMe_2SiH with both **3** and **4** proceed without fragmentation of the cluster framework to give novel di- or trinuclear silyl-ruthenium complexes with unique structures, **6** and **7**, respectively (Scheme 3). Of importance is that the triruthenium silyl complex **6** has been shown to be a better catalyst than **3**. Monitoring the catalytic hydrosilylation using **6** revealed that **6** is converted to other species during the reaction, whereas it is regenerated completely after the reaction is completed. This offers interesting evidence for the involvement of cluster species in the catalytic hydrosilylation.

Results and Discussion

Comparison of the Catalytic Activity of 1, 3, 4, and 5 in the Hydrosilylation of Acetophenone. As noted above, complexes bearing a bridging acenaphthylene or 4,6,8-trimethylazulene ligand catalyze the hydrosilylation of acetophenone at room temperature. In the presence of a catalytic amount (1 mol %) of **1**, **3**, **4**, or **5**, hydrosilylation of acetophenone in benzene was carried out. The results are shown in Table 1. When $\text{HSiMe}_2(\text{CH}_2)_2\text{Me}_2\text{SiH}$ is used as the silane, the yield of the silyl ether reaches 91% after 1.5 h with **1** as a catalyst. In contrast, the reaction with **3** is slower (31% yield after 1.5 h and 89% after 20 h), whereas **5** is inactive. Although the reaction is much slower, some acetophenones are hydrosilylated by **4**. The reactions with PhMe_2SiH in the presence of **1** or **3** are slower than those with $\text{HSiMe}_2(\text{CH}_2)_2\text{Me}_2\text{SiH}$;¹² the yield of the silyl ether with **1** as a catalyst reaches over 91% after 9 h, whereas only 52% yield is obtained after 12 h with **3**. These results suggest that the catalytic activity of triruthenium clusters **1** and **3** toward hydrosilylation of acetophenone is higher than that of the others. Since an oxidative addition of R_3SiH to metallic species is believed to be involved in the initial step of the catalytic hydrosilylation, the reaction of R_3SiH with transition metal complexes has been investigated by isolation of the products, which possess silyl–metal bonds.¹ The analysis of metal species involved in slow catalytic

reactions sometimes provides important information on the net catalytically active species.³ Within this context, we examined the stoichiometric reaction of **3** with PhMe_2SiH . In a closely related reaction, we achieved the isolation of a silyl-ruthenium cluster **2** from **1**, as described earlier.¹²

Reaction of 3 with PhMe_2SiH . Treatment of **3** with PhMe_2SiH (5 equiv to 1 equiv of **3**) in benzene- d_6 at 40 °C for 16 h results in the formation of a novel silyl-ruthenium complex ($\mu_2, \eta^3: \eta^5$ -4,6,8-trimethyl-4,5-dihydroazulene) $\text{Ru}_3(\text{H})(\text{CO})_6(\text{SiMe}_2\text{Ph})$ (**6**) in 50% yield (Scheme 3, eq 1). As reported earlier, reaction of **1** with HSiMe_2Ph proceeds at 80 °C to form **2**.¹² In sharp contrast, the reaction of **3** to **6** proceeds even at room temperature, at which the catalytic hydrosilylation of acetophenone occurs. In other words, the silyl ruthenium complexes **6** can be generated in the actual catalytic reaction.

Spectral data of **6** are listed in Table 2. The ^1H NMR spectrum of **6** shows a singlet at $\delta -13.6$ assignable to a bridging Ru–H. Existence of a Ru– SiMe_2Ph moiety is suggested by ^1H resonances ($\delta_{\text{H}} 0.57$ and 0.61) as two singlets due to the diastereotopic SiMe groups and peaks from $\delta_{\text{H}} 6.96$ –7.02 to 7.30–7.33 due to the SiPh moiety) and a single ^{29}Si resonance ($\delta 43.18$).¹⁴ Six peaks observed at $\delta_{\text{C}} 192$ –213 in the ^{13}C NMR spectrum and six ν_{CO} absorptions seen in the IR spectrum indicate the presence of six CO ligands. An IR absorption with a relatively low wavenumber (1885 cm^{-1}) indicates that one of the CO ligands should be bridging two ruthenium centers.¹⁵ ^1H and ^{13}C resonances due to the azulene moiety have been assigned completely with the aid of the H–H and H–C COSY techniques. Five ^1H (H1–H5) and eight ^{13}C (C1–C6, C9, C10) resonances show a typical upfield shift due to the fact that these carbons are bonded to the metal centers. Multiplets consisting of three protons, appearing at $\delta_{\text{H}} 0.74$ –0.93, and a doublet at $\delta_{\text{H}} 0.57$, due to a methyl group, suggest the existence of a CH_3 – CH – CH_2 – moiety in the azulene ligand. In other words, one carbon–carbon double bond in the azulene ligand in the precursor **3** is hydrogenated during the reaction.

These spectral features of **6** are consistent with the molecular structure derived from an X-ray single-crystal structure determination as illustrated in Figure 2.¹⁵ The crystallographic data are shown in Table 3, and the representative bond distances and angles are listed in Table 4. The compound **6** possesses a triruthenium framework with Ru–Ru distances of 2.905(1), 2.891(1), and 2.761(1) Å. A PhMe_2Si moiety is bonded to the Ru(3) atom with a Ru–Si distance of 2.392(2) Å. Six CO ligands are bound to the cluster, and each ruthenium atom has two CO ligands. The relatively short Ru(3)–C(15) distance (2.658(10) Å) and the Ru(1)–C(15)–O(1) angle of $164.6(10)^\circ$ provide evidence for a semibridging interaction of this CO ligand between Ru(1) and Ru(3)

(14) Multiruthenium complexes having H–Ru–Si moieties reportedly show peaks due to the bridging hydride at $\delta -9$ to -17 , whereas these compounds provide the ^{29}Si signals at $\delta 10$ –60: Corey, J. Y.; Braddock-Wilking, D. *Chem. Rev.* **1999**, *99*, 175.

(15) A bridging hydride ligand across the Ru(2) and Ru(3) atoms was visible in the difference Fourier map after refinement, but could not be refined because the quality of the data was not very good.

Scheme 3

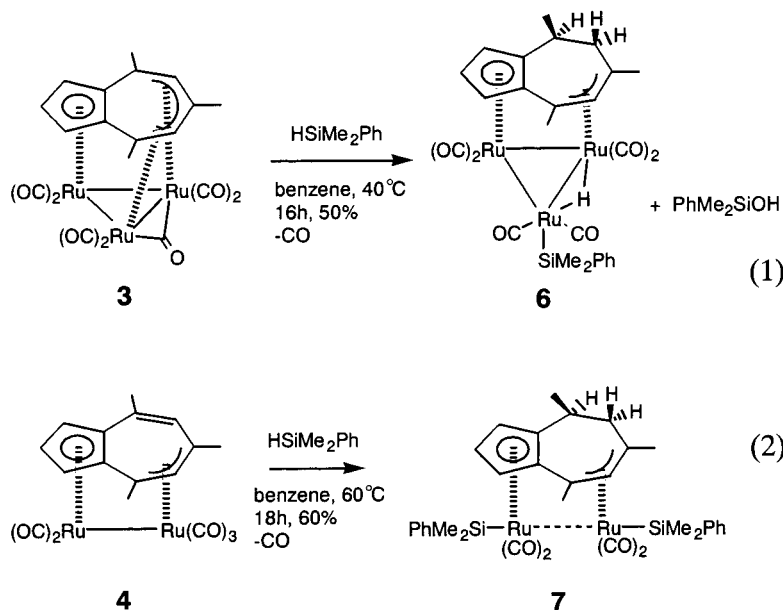
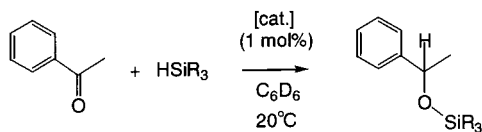


Table 1. Hydroarylation of Acetophenone with [HSiMe₂CH₂]₂ and PhMe₂SiH Catalyzed by 1, 3, 4, and 5



entry	catalyst	hydrosilane	time (h)	yield (%) ^b
1	1	[HSiMe ₂ CH ₂] ₂	1.5	91
2	3	[HSiMe ₂ CH ₂] ₂	1.5	31
			21	89
3	4	[HSiMe ₂ CH ₂] ₂	1.5	1
			35	12
4	5	[HSiMe ₂ CH ₂] ₂	1.5	0
			30	2
5	1	PhMe ₂ SiH	9	91
6	3	PhMe ₂ SiH	12	52

^a All reactions have been carried out using 1 mol % of the catalysts, **1**, **3**, **4**, or **5**, in a 5 mm ϕ NMR tube in benzene-*d*₆ at 20 °C. ^b Yields of the products were determined by ¹H NMR spectroscopy, based on the integral value of the internal standard (1,2-dichloroethane).

atoms.¹⁶ Cp-like coordination of the carbons in the five-membered ring to the Ru(1) atom and a η^3 -allyl interaction of the three carbons in the seven-membered ring with the Ru(2) atom bring about the $\mu_2, \eta^3: \eta^5$ -coordination mode of the dihydroazulene ligand to the triruthenium framework.

As described in our previous paper, reaction of **1** with trialkylsilanes results in dissociation of a CO ligand followed by oxidative addition of a Si–H bond to afford the silyl cluster **2**.¹² A major difference of the structure of **6** from that of **2** is the coordination mode of the

conjugated π -ligand. Both **2** and **6** have the Ru(H)(SiR₃)(CO)₆ moiety, and the acenaphthylene ligand in **2** acts as a triply bridging 10-electron donor to the cluster moiety. In contrast, the dihydroazulene ligand in **6** behaves as a doubly bridging eight-electron donor ligand. As a consequence, the total electron count of **6** is 46 (that of **2** is 48), and the Ru(H)(SiR₃)(CO)₆ moiety in **6** is coordinatively unsaturated. The 46-electron cluster is formally rationalized by the existence of a Ru–Ru double bond.¹⁷ The Ru(2)–Ru(3) bond length of 2.761(1) Å, which is slightly shorter than the other two Ru–Ru distances, may be responsible for the double bonded nature of Ru(2)–Ru(3), though it is in the range of the usual Ru–Ru single bond distance in other clusters.¹⁸ The semibridging interaction of a carbonyl ligand may mitigate the unsaturated nature of the metal centers in **6**.¹⁹ There have been some early examples of unsaturated clusters or their equivalents in osmium chemistry, and one of the more famous examples is the 46-electron cluster [Os₃H₂(CO)₁₀], which is known to undergo a number of reactions.²⁰ Coordinatively unsaturated triruthenium clusters are not as common, compared to the triosmium analogues, and **6**

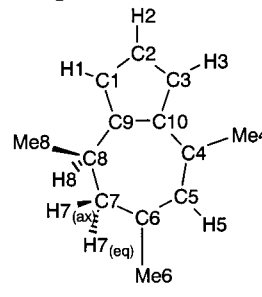
(17) (a) Metal–metal multiple bonds and coordinative unsaturation of clusters, see: *Compounds with Multiple Bonds Between Metal Atoms*; Cotton, F. A., Walton, R., Wiley: New York, 1980. (b) Recent reports about coordinatively unsaturated clusters having metal–metal double bonds: Süss-fink, G.; Godefroy, I.; Ferrand, V.; Neels, A.; Stoeckli-Evans, H. *J. Chem. Soc., Dalton Trans.* **1998**, 515; Bruce, M. I.; Skelton, B. W.; White, A. H.; Zaitseva, N. N. *J. Chem. Soc., Dalton Trans.* **1999**, 1445.

(18) Usual Ru–Ru bond distances in triruthenium carbonyl clusters, for example, [Ru₃(CO)₁₂],^{19a} ($\mu_2, \eta^5: \eta^5$ -guaiazulene)Ru₃(CO)₇,^{19b} and **1**,^{18b} are in the range 2.7–3.0 Å: (a) Churchill, M. R.; Hollander, F. J.; Hutchinson, J. P. *Inorg. Chem.* **1977**, *16*, 2655. (b) Johnson, B. F. G.; Shephard, D. S.; Edwards, A. J.; Braga, D.; Parisini, E.; Raithby, P. R. *J. Chem. Soc., Dalton Trans.* **1995**, 3307.

(19) Examples of unsaturated complexes having semibridging CO ligands, see: (a) Field, J. S.; Haines, R. J.; Mulla, F. *J. Organomet. Chem.* **1990**, *389*, 227. (b) Field, J. S.; Haines, R. J.; Stewart, M. W.; Sundermeyer, J.; Woollam, S. F. *J. Chem. Soc., Dalton Trans.* **1993**, 947.

(20) For reviews: (a) Deeming, A. J. *Adv. Organomet. Chem.* **1986**, *26*, 1. (b) Deeming, A. J. In *Comprehensive Organometallic Chemistry II*; Wilkinson, G., Stone, F. G. A., Abel, E. W., Eds.; Pergamon: Oxford, Vol. 7, Chapter 12.

(16) Semibridging CO ligands can be identified by means of X-ray crystallography or IR spectra. The absorption due to the semibridging CO ligands is generally observed at 1850–1900 cm⁻¹, which is lower than those of usual terminal CO ligands, for example: (a) Curtis, M. D.; Han, K. R.; Butler, W. M. *Inorg. Chem.* **1980**, *19*, 2096. (b) Sterenberg, B. T.; Jennings, M. C.; Puddephatt, R. J. *Organometallics* **1999**, *18*, 2162. (c) Oke, O.; McDonald, R.; Cowie, M. *Organometallics* **1999**, *18*, 1629. (d) Baxter, R. J.; Knox, G. R.; Pauson, P. L.; Spicer, M. D. *Organometallics* **1999**, *18*, 215. (e) Cotton, F. A. *Prog. Inorg. Chem.* **1976**, *21*, 1, and reference therein.

Table 2. Spectral Data of **6** and **7**^a


	6	7
¹ H (δ)		
RuH	-13.6 (s)	
H1	4.35 (dd, <i>J</i> = 1.8, 2.7 Hz)	3.87 (dd, <i>J</i> = 1.9, 2.9 Hz)
H2	4.37 (t, <i>J</i> = 2.7 Hz)	3.95 (t, <i>J</i> = 2.9 Hz)
H3	2.29 (dd, <i>J</i> = 1.8, 2.7 Hz)	3.50 (dd, <i>J</i> = 1.9, 2.9 Hz)
H5	5.22 (s)	4.99 (s)
H7(eq) ^b	0.93 (m)	2.06 (dd, <i>J</i> = 4.9, 16.6 Hz)
H7(ax) ^b	0.93 (m)	1.52 (dd, <i>J</i> = 2.2, 16.6 Hz)
H8 ^b	0.74 (m)	0.9 (m)
Me4	1.75 (s)	1.64 (s)
Me6	1.20 (s)	1.31 (s)
Me8	0.57 (d, <i>J</i> = 7.1 Hz)	0.59 (d, <i>J</i> = 7.1 Hz)
SiMe	0.57 (s), 0.61 (s)	0.84 (s), 0.88 (s), 0.95 (s), 0.97 (s)
SiPh	6.96–7.02 (3H) 7.30–7.33 (2H)	7.78 (dd, <i>J</i> = 1.3, 7.9 Hz, 2H) 7.57 (dd, <i>J</i> = 1.3, 7.9 Hz, 2H) 7.16–7.32 (6H)
¹³ C{ ¹ H} (δ)		
C1	81.7	87.7
C2	86.0	85.0
C3	80.5	88.5
C4	63.8	81.4
C5	96.0	100.9
C6	70.4	70.7
C7	50.1	53.5
C8	28.1	29.1
C9	101.7	112.2
C10	88.7	63.5
Me4	25.3	23.1
Me6	33.7	32.5
Me8	20.4	18.6
SiMe	5.8, 7.6	5.9, 6.1, 7.0, 8.0
SiPh	133.6, 146.3	132.3, 133.8, 146.9, 147.8
CO	192.5, 195.6, 199.8, 204.7, 208.3, 213.2	199.0, 200.0, 203.4, 209.4
²⁹ Si (δ) ^c	43.2	22.3, 27.4
IR (cm ⁻¹) ^d ν _{CO}	2048, 2023, 1972, 1941, 1911, 1885	2048, 2014, 1955, 1920

^a Measured in benzene-*d*₆ at room temperature. The numbering of the protons and carbons in 4,6,8-trimethyl-4,5-dihydroazulene ligand is shown above. ^b Two hydrogen atoms bonded to C(7) were located at equatorial (eq) and axial (ax) positions. They were assigned on the basis of NOE, ¹H–¹H COSY, and HMQC NMR measurements. ^c The ²⁹Si NMR measurements were carried out using INEPT technique. ^d IR spectra were recorded using KBr tablets.

is a rare example of a completely characterized unsaturated triruthenium cluster.²¹

As pointed out earlier, the reaction of **3** with PhMe₂-SiH involves hydrogenation of a carbon–carbon double bond in the azulene ligand of **3**. The hydrogenation

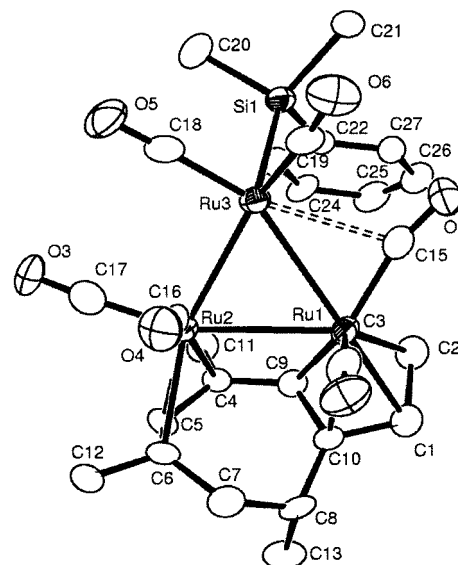


Figure 2. Perspective drawing of **6**, (*μ*₂,*η*³:*η*⁵-4,6,8-trimethyl-4,5-dihydroazulene)Ru₃(H)(CO)₆(SiMe₂Ph) with 50% probability thermal ellipsoids.

Table 3. Crystal Data and Structure Refinement for **6** and **7**

	6	7
empirical formula	C ₂₇ H ₂₈ O ₆ Ru ₃ Si	C ₃₃ H ₃₈ O ₄ Ru ₂ Si ₂
fw	779.90	756.95
temperature, K	293(2)	293(2)
wavelength, Å	0.71069	0.71069
cryst syst	triclinic	orthorhombic
space group	<i>P</i> 1	<i>P</i> 2 ₁ 2 ₁ 2 ₁
<i>a</i> , Å	10.990(3)	16.701(4)
<i>b</i> , Å	14.709(5)	20.81(2)
<i>c</i> , Å	9.685(3)	9.530(2)
α, deg	93.816(12)	90
β, deg	112.652(6)	90
γ, deg	77.36(2)	90
<i>V</i> , Å ³	1409.6(8)	3312(3)
<i>Z</i>	2	8
<i>D</i> (calcd), Mg/m ³	1.835	1.518
abs coeff, mm ⁻¹	1.668	1.018
<i>F</i> (000)	766	1536
cryst size, mm	0.50 × 0.40 × 0.20	0.38 × 0.18 × 0.15
θ range, deg	2.84 to 27.47	2.63 to 30.00
no. of indep reflns	4960	5391
no. of reflns collected	4960 [<i>R</i> _{int} = 0.00]	5360 [<i>R</i> _{int} = 0.00]
no. of reflns obsd (>2σ)	3609	3188
no. of data/restraints/params	4660/0/334	5360/0/370
goodness-of-fit ^a on <i>F</i> ²	0.973	1.028
<i>R</i> indices [<i>I</i> > 2σ(<i>I</i>)] ^b	<i>R</i> ₁ = 0.0682 <i>wR</i> ₂ = 0.1613	<i>R</i> = 0.0588 <i>wR</i> ₂ = 0.0966
<i>R</i> indices (all data) ^c	<i>R</i> ₁ = 0.0926 <i>wR</i> ₂ = 0.1833	<i>R</i> = 0.1329 <i>wR</i> ₂ = 0.1152
larg diff peak & hole, e Å ⁻³	1.054 and -1.589	0.626 and -0.638

^a GOF = [Σ*w*(*F*_o² - *F*_c²)/Σ(*N* - *P*)]^{1/2}. ^b *R*(*F*) = Σ||*F*_o|| - ||*F*_c||/Σ||*F*_o||. ^c *wR*(*F*₂) = [Σ*w*(*F*_o² - *F*_c²)/Σ*w*(*F*_o²)]^{1/2}.

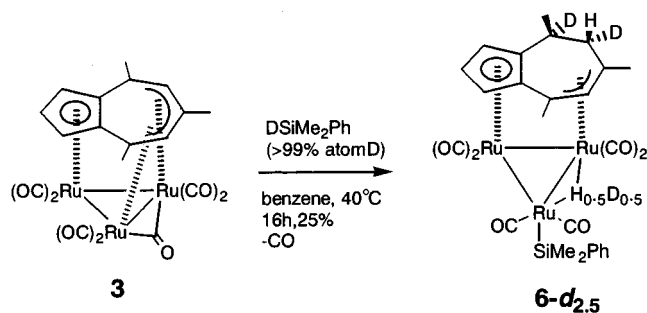
produces a sp³ carbon (C8). The methyl group bound to the C(8) atom is located at the face of the azulene plane opposite the triruthenium moiety. This indicates that the addition of hydrogen atoms occurs from the direction of the triruthenium moiety. The reaction of PhSiMe₂D with **3** leads to the addition of two deuterium atoms to the C(7) and C(8) carbons (**6-d**), and their *cis*-configuration was confirmed by the NOE enhancement between Me(8) and H(7) (Scheme 4).²² Thus, at least two molecules of PhMe₂SiH react with **3** and take part in

(21) Examples of coordinatively unsaturated triruthenium carbonyl clusters: (a) Hutchins, L. D.; Duesler, E. N.; Paine, R. T. *Organometallics* **1984**, *3*, 399. (b) Nagashima, H.; Fukahori, T.; Aoki, K.; Itoh, K. *J. Am. Chem. Soc.* **1993**, *115*, 10430. (c) Field, J. S.; Haines, R. J.; Mulla, F. *J. Organomet. Chem.* **1992**, *439*, D56. (d) Knox, S. A. R.; Koepke, J. W.; Andrews, M. A.; Kaesz, H. D. *J. Am. Chem. Soc.* **1975**, *97*, 3942.

Table 4. Representative Bond Distances and Angles in 6

Bond Distances (Å)			
Ru(1)–Ru(2)	2.9048(14)	Ru(1)–Ru(3)	2.8908(14)
Ru(2)–Ru(3)	2.7605(13)	Ru(3)–Si(1)	2.392(2)
Ru(1)–C(1)	2.286(10)	Ru(1)–C(2)	2.260(11)
Ru(1)–C(3)	2.289(11)	Ru(1)–C(9)	2.312(10)
Ru(1)–C(10)	2.270(9)	Ru(2)–C(6)	2.270(9)
Ru(2)–C(7)	2.206(10)	Ru(2)–C(8)	2.257(9)
Ru(1)–C(14)	1.853(10)	Ru(1)–C(15)	1.879(10)
Ru(2)–C(17)	1.869(12)	Ru(2)–C(16)	1.925(11)
Ru(3)–C(19)	1.851(10)	Ru(3)–C(18)	1.852(12)
C(15)–O(1)	1.153(12)	C(14)–O(2)	1.164(12)
C(17)–O(3)	1.141(14)	C(16)–O(4)	1.146(13)
C(18)–O(5)	1.165(14)	C(19)–O(6)	1.186(13)

Bond Angles (deg)			
Ru(1)–Ru(2)–Ru(3)	61.30(3)	Ru(1)–Ru(3)–Ru(2)	61.81(3)
Ru(2)–Ru(1)–Ru(3)	56.89(3)	Ru(1)–Ru(3)–Si(1)	113.86(8)
Ru(2)–Ru(3)–Si(1)	123.60(7)	Ru(1)–C(14)–O(2)	174.4(10)
Ru(1)–C(15)–O(1)	164.6(10)	Ru(2)–C(16)–O(4)	168.4(9)
Ru(2)–C(17)–O(3)	176.3(10)	Ru(3)–C(18)–O(5)	174.8(11)
Ru(3)–C(19)–O(6)	174.1(10)	C(10)–C(4)–C(5)	115.3(8)
C(4)–C(5)–C(6)	118.7(8)	C(5)–C(6)–C(7)	125.3(10)
C(6)–C(7)–C(8)	127.2(8)	C(7)–C(8)–C(9)	121.7(8)

Scheme 4

the hydrogenation of the azulene ligand, presumably via formation of two ruthenium hydrides by activation of these silanes with ruthenium clusters, followed by transfer of these hydrides from the metal centers to the azulene ligand. Similar reaction pathways, i.e., the oxidative addition of two molecules of PhMe_2SiH to the diruthenium species and subsequent transfer of the resulting ruthenium-hydrides to the azulene ligand, are seen in the reaction of **4** to **7** (vide infra). Analysis of the organic products in the reaction mixture reveals the formation of PhMe_2SiOH ; this suggests that one of the PhMe_2Si groups in the disilyl intermediate has been removed by reaction with trace amounts of water contained in the reaction medium to form **6**. A possible mechanism is shown in Scheme 5.²³

Reaction of 4 with PhMe_2SiH . Since the diruthenium compound **4** shows some catalytic activity in the hydrosilylation of acetophenone, we considered it worthwhile to examine the reaction of **4** with HMe_2SiPh to compare it to that of **3**. Reaction of **4** with HMe_2SiPh (5 equiv to **4**) for 18 h in benzene at 60 °C gives a disilylated ruthenium complex **7** in 60% yield (Scheme 3, eq 2). The spectral data of **7** are listed in Table 2. This new complex has no Ru–H signal in ^1H NMR and two resonances in ^{29}Si NMR (δ 22.3 and 27.4). Four ^{13}C resonances at δ_{C} 199–209 and the same number of ν_{CO}

(22) Using DSiMe_2Ph (99% *d*), deuterium contents in H(7)(eq) and H(8) of the dihydroazulene ligand were >95%, which were determined by ^1H and ^2H NMR measurements. Details are shown in the Supporting Information.

absorptions indicate the existence of four-coordinated COs. The upfield shift of ^1H and ^{13}C resonances due to H1–H5 and C1–C6, C9, and C10 suggests the coordination of these eight carbons to the diruthenium moiety. Other ^1H and ^{13}C resonances similar to those observed in **7** indicate the existence of a 4,5-dihydro-4,6,8-trimethylazulene ligand similar to **6**.

The molecular structure of **7** as determined by X-ray single-crystal structural analysis supports all of these spectral features, as shown in Figure 3. Crystallographic data are shown in the right-hand column of Table 3, and representative bond distances and angles are listed in Table 5. The molecule contains two ruthenium atoms, and each ruthenium atom has two CO ligands and one PhMe_2Si group. The Ru–Si bond lengths are 2.442(3) and 2.404(3) Å. The dihydroazulene ligand is bound to the diruthenium moiety in the μ_2, η^3, η^5 -coordination mode. An important feature of this diruthenium compound is the electron configuration of both ruthenium atoms; the Ru(1) species has an 18-electron configuration, whereas the Ru(2) moiety has a 16-electron configuration. The Ru–Ru distance of 3.141(2) Å is longer than the usual Ru–Ru bond length in diruthenium carbonyl complexes,²⁴ but it is still within bonding distance.²⁵ This suggests the existence of a Ru(1)→Ru(2) dative bond. Ru→Ru dative bonds are not common in diruthenium carbonyl complexes, but are seen in two diruthenium complexes, $(\text{Cl}_3\text{Si})_2(\text{CO})_4(\text{PMe}_3)\text{Ru} \rightarrow \text{Ru}(\text{CO})_3(\text{SiCl}_3)_2$ [Ru–Ru = 2.995(1) and 2.975(1) Å] and $(\text{Cl}_3\text{Si})_2(\text{CO})_3(\text{tBuNC})_2\text{Ru} \rightarrow \text{Ru}(\text{CO})_3(\text{SiCl}_3)_2$ [Ru–Ru = 2.9488(2) Å], reported by Pomeroy and co-workers.²⁶

Similar to the formation of **6** from **3**, the reaction of **4** with PhMe_2SiH is accompanied by hydrogenation of a carbon–carbon double bond in the azulene ligand in **4**. Experiments using PhMe_2SiD revealed the introduction of two deuterium atoms in the dihydroazulene ligand in **7** (Scheme 6). The stereochemical analysis of the C(8) carbon in the X-ray crystal structure shows that the Me(8) group is located at the side opposite the diruthenium moiety. The *cis*-configuration of the two deuterium atoms was determined by ^1H NOE experiments of Me(8) and C(7)–H in **7**. This suggests that hydrogen or deuterium atoms, activated by diruthenium species, contribute to the formation of the dihydro- or dideuterioazulene ligand. Although further studies are required to clarify the reduction mechanism, one of the plausible schemes is shown in Scheme 7. An alternation of the coordination mode from μ_2, η^3, η^5 - to μ_2, η^1, η^5 - is seen in

(23) The deuterium content in the hydride ligand of **6-d** formed by the reaction of **3** with PhMe_2SiD was 50%. This suggests existence of H/D exchange processes with Ru–H and PhMe_2SiD , though the mechanism is not clear at present.

(24) Usual Ru–Ru bond distances in diruthenium carbonyl complexes, for example, $(\mu_2, \eta^3, \eta^5\text{-guaiazulene})\text{Ru}_2(\text{CO})_5$: 2.8795(5) and 2.894(2) Å,^{24a} $(\mu_2, \eta^3, \eta^5\text{-4,6,8-trimethyl azulene})\text{Ru}_2(\text{CO})_5$: 2.8603(8) Å,^{24b} $(\mu, \eta^1, \eta^2, \eta^2, \eta^3\text{-Me}_2\text{SiCH}_2\text{CH}_2\text{SiMe}_2\text{C}_8\text{H}_8)\text{Ru}_2(\text{CO})_5$: 2.9340(5) Å.^{24c} (a) Matsubara, K.; Oda, T.; Nagashima, H. *Organometallics* **2001**, *20*, 881. (b) Matsubara, K.; Tsuchiya, K. Mima, S.; Nagashima, H. Unpublished data. (c) Goddard, R.; Woodward, P. *J. Chem. Soc., Dalton Trans.* **1980**, 559.

(25) Certain ruthenium clusters have Ru–Ru bonds of which distances are as long as 3.2 Å: (a) Hogarth, G.; Phillips, J. A.; Van Gastel, F.; Taylor, N. J.; Marder, T. B.; Carty, A. J. *J. Chem. Soc., Chem. Commun.* **1988**, 1570. (b) Johnson, B. F. G.; Lewis, J.; Mace, J. M.; Raithby, P. R.; Vargas, M. D. *J. Organomet. Chem.* **1987**, *321*, 409.

(26) Diruthenium carbonyl complexes having M–M dative bonds: Jiang, F.; Male, J. L.; Bradha, K.; Leong, W. K.; Pomeroy, R. K.; Zaworotko, M. J. *Organometallics* **1998**, *17*, 5810.

Scheme 5

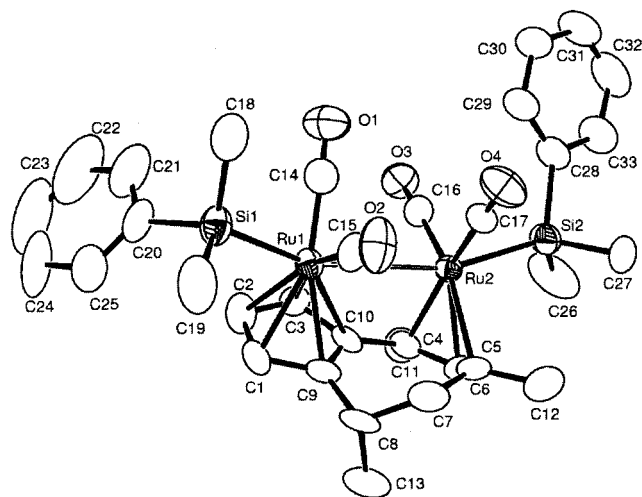
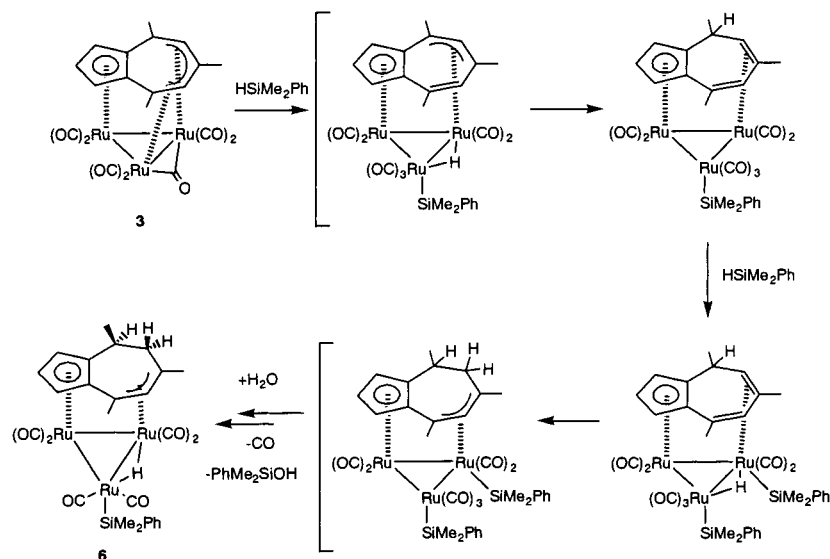


Figure 3. Perspective drawing of **7**, ($\mu_2, \eta^3: \eta^5$ -4,6,8-trimethyl-4,5-dihydroazulene) $\text{Ru}_2(\text{CO})_4(\text{SiMe}_2\text{Ph})_2$ with 50% probability thermal ellipsoids.

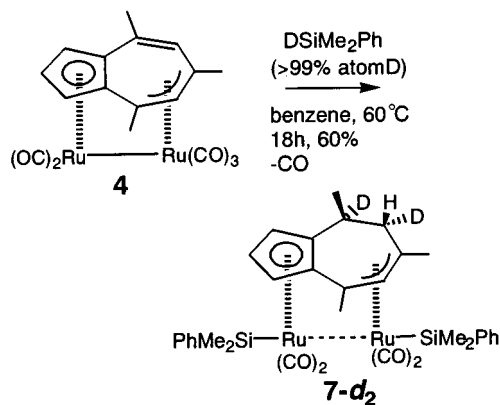
the reaction of ($\mu_2, \eta^3: \eta^5$ -guaiazulene) $\text{Ru}_2(\text{CO})_5$ with phosphorus^{24a} or isonitrile ligands.²⁷

Catalytic Hydrosilylation of Ketones with $\text{PhMe}_2\text{-SiH}$ Using the Silyl Complexes **6 and **7**.** Possible catalytic cycles for hydrosilylation of unsaturated molecules have been well investigated both experimentally and theoretically, and one of the plausible catalytic cycles is illustrated in Scheme 8a.¹ The oxidative addition of H-Si to metallic species to form H-M-Si species is believed to initiate the catalytic cycle. In the $\text{Co}_2(\text{CO})_8$ -catalyzed hydrosilylation of olefins, the Si-Co species formed by the reaction of $\text{Co}_2(\text{CO})_8$ with trialkylsilanes is involved in the catalytic cycle as shown in Scheme 8b.⁵ The silyl-hydride cluster **6** may be considered as a related species to the catalytically active H-M-Si species shown in Scheme 8a, whereas the disilyldiruthenium complex **7** may be an analogue of the Si-Co species, shown in Scheme 8b. Starting from these analogies, we were interested in whether **6** and **7** may be intermediates in the catalytic hydrosilylation. It has

Table 5. Representative Bond Distances and Angles in **7**

Bond Distances (Å)			
Ru(1)-Ru(2)	3.141(2)	Ru(1)-Si(1)	2.442(3)
Ru(2)-Si(2)	2.404(3)	Ru(1)-C(1)	2.24(1)
Ru(1)-C(2)	2.245(9)	Ru(1)-C(3)	2.250(9)
Ru(1)-C(9)	2.290(9)	Ru(1)-C(10)	2.40(1)
Ru(2)-C(5)	2.189(9)	Ru(2)-C(4)	2.201(9)
Ru(2)-C(6)	2.314(9)	Ru(1)-C(14)	1.86(1)
Ru(1)-C(15)	1.87(1)	Ru(2)-C(17)	1.868(9)
Ru(2)-C(16)	1.869(9)	C(14)-O(1)	1.15(1)
C(15)-O(2)	1.14(1)	C(16)-O(3)	1.15(1)
C(17)-O(4)	1.15(1)		
Bond Angles (deg)			
Ru(2)-Ru(1)-Si(1)	156.70(8)	Ru(2)-Ru(1)-C(14)	81.3(3)
Ru(2)-Ru(1)-C(15)	82.7(3)	Ru(1)-Ru(2)-Si(2)	162.63(8)
Ru(1)-Ru(2)-C(16)	85.4(3)	Ru(1)-Ru(2)-C(17)	90.3(3)
C(14)-Ru(1)-C(15)	89.2(4)	Si(2)-Ru(2)-C(17)	81.9(3)
Si(2)-Ru(2)-C(16)	81.6(3)	Ru(1)-C(14)-O(1)	177(1)
Ru(1)-C(15)-O(2)	176.3(9)	Ru(2)-C(16)-O(3)	175(1)
Ru(2)-C(17)-O(4)	178.6(9)	C(5)-C(4)-C(10)	121.1(9)
C(4)-C(5)-C(6)	126.5(9)	C(5)-C(6)-C(7)	124.4(9)
C(6)-C(7)-C(8)	119.4(9)	C(7)-C(8)-C(9)	113.0(8)

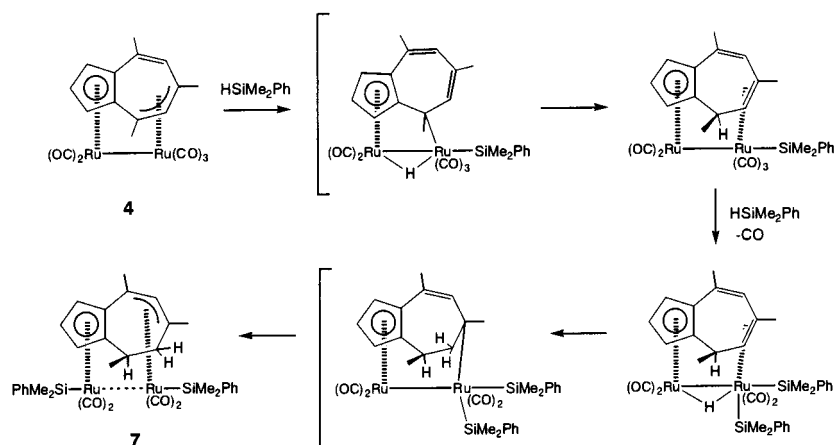
Scheme 6



been noted above that the silyl-hydride cluster **6** is a 46-electron compound and coordinatively unsaturated. The disilyldiruthenium complex **7** possibly forms an unsaturated species with the cleavage of the dative Ru-Ru bond. These unsaturated species may provide higher activity to **6** and **7** in the catalytic hydrosilylation of acetophenone than in the cases of **3** and **4**.

(27) Matsubara, K.; Mima, S.; Oda, T.; Nagashima, H. *J. Organomet. Chem.* **2002**, *650*, 96.

Scheme 7



Scheme 8

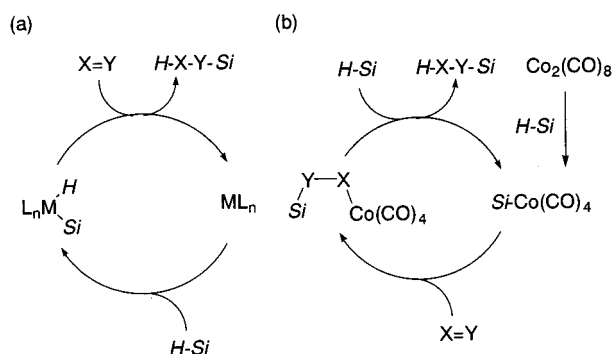
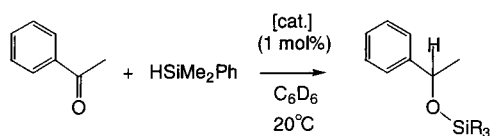


Table 6. Hydrosilylation of Acetophenone with HSiMe₂Ph Catalyzed by **3, **6**, and **7****



entry	catalyst	time (h)	yield (%) ^b
1	3	12	52
2	6	12	100
4	7	12	0

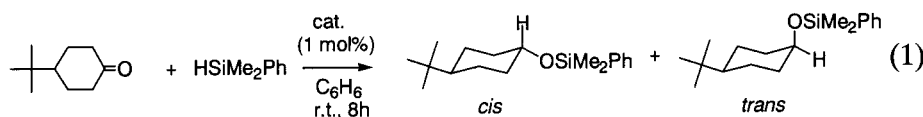
^a All reactions were carried out using 1 mol % of catalysts **3**, **6**, or **7** in a 5 mm ϕ NMR tube in benzene-*d*₆ at 20 °C. ^b Yields of the products were determined by ¹H NMR spectroscopy, based on the integral value of the internal standard (1,2-dichloroethane).

A mixture of acetophenone, HSiMe₂Ph (1 equiv of HSiMe₂Ph to 1 equiv of acetophenone), and a catalytic amount of **6** or **7** (1 mol % to acetophenone) was dissolved in C₆D₆, and the reaction was monitored periodically using ¹H NMR. Although **7** was inactive, **6** revealed higher activity in the catalytic hydrosilylation of acetophenone than the precursor **3**, as shown in Table 6. After 12 h, all of the charged acetophenone was consumed in the reaction using **6**, whereas the conversion was 52% in the reaction catalyzed by **3** under the same conditions. Hydrosilylations of 4-*tert*-butylcyclohexanone and mesityl oxide were also catalyzed by **6**. Comparable experiments with **1** and **3** as the catalysts revealed that yields of the products after 8 h (4-*tert*-butylcyclohexanone) and 12 h (mesityl oxide) at room temperature are in the order **6** > **1**, **3**. Only small differences were observed in the *cis/trans* ratios of the

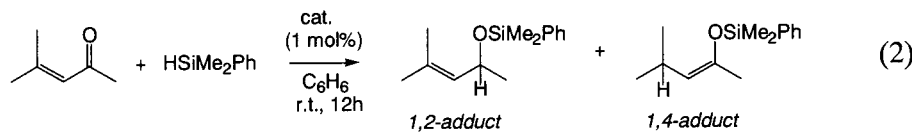
silyl ether of 4-*tert*-butylcyclohexanol (Scheme 9, eq 1) and in the ratios of 1,4- to 1,2-addition product from mesityl oxide (Scheme 9, eq 2).¹²

Further investigation to see intermediary species in the catalytic hydrosilylation of acetophenone by ¹H NMR provided interesting time-dependent NMR spectra as shown in Figure 4. To a solution of **6** (0.1 equiv to 1.0 equiv of acetophenone) in C₆D₆ were added acetophenone and HSiMe₂Ph (0.9 equiv to 1.0 equiv of acetophenone), and the ¹H NMR spectrum of this solution was monitored periodically. At the initial stage (after 0.1 h of the addition (Figure 4a), where no reaction of acetophenone has taken place, the ¹H NMR spectrum of the metal hydride region shows a Ru-H signal of **6** at $\delta_{\text{H}} = 13.6$ as a single peak. After 0.5 h, 52% of acetophenone and 51% of PhMe₂SiH have been consumed. At this stage, the peak intensity at $\delta_{\text{H}} = 13.6$ (Ru-H of **6**) has decreased significantly, and several other hydride signals appear, including a Ru-H at $\delta_{\text{H}} = 10.0$ as a major peak (Figure 4b). After 12 h, 92% of acetophenone and all of the PhMe₂SiH have been converted to the corresponding silyl ether. At this stage (Figure 4c), the peak at $\delta_{\text{H}} = 13.6$ is regenerated and can be observed as almost one peak. Analysis of the other ¹H resonances reveals that at the initial stage only the peaks due to unreacted acetophenone, PhMe₂SiH, and **6** can be observed, whereas at the final stage, only the signals attributed to unreacted acetophenone (~8%), PhMe₂SiO(CH₃)-CHPh (92%), and **6** are visible. The peak intensity of the signal at $\delta_{\text{H}} = 13.6$, when compared with that of the solvent signal, is almost identical before and after the reaction. The results unequivocally show that the cluster **6** reacts with acetophenone and HSiMe₂Ph to form some kind of catalytic intermediates as transient species during the reaction and is regenerated after all of the hydrosilane has been converted (Figure 4c). As has been described in the Introduction, cluster compounds often undergo fragmentation of the cluster framework in the reaction with HSiR₃, leading to alternation of the nuclearity. Once the cluster framework is fragmented, its complete re-formation from the fragmentation products to the original cluster is difficult. Therefore, the present observation suggests that the intermediates of the catalytic hydrosilylation should contain the triruthenium framework derived from **6**; thus the cluster species should be involved in the catalytic cycle.²⁸

Scheme 9



catalyst;	1:	yield 10 %,	cis/trans = 67 / 33
	3:	10 %,	60 / 40
	6:	28 %,	67 / 33



catalyst;	1:	yield 37 %,	1,2/1,4 = 67 / 33
	3:	19 %,	67 / 33
	6:	50 %,	70 / 30

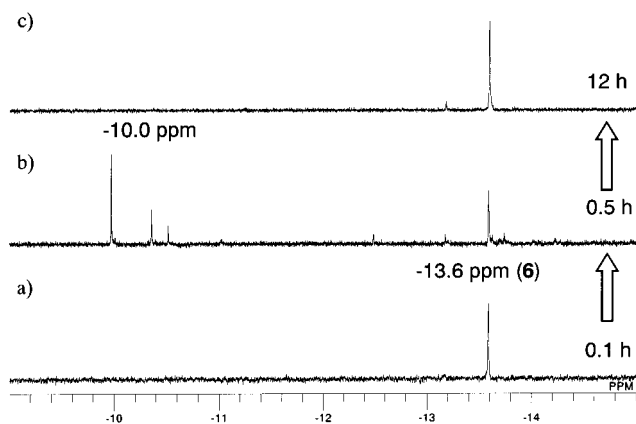


Figure 4. ^1H NMR spectra (the hydride region) in the hydrosilylation of acetophenone catalyzed by **6**. (a) After 0.1 h, no reaction has taken place. (b) After 0.5 h, 52% of acetophenone and 51% of HSiMe_2Ph have been converted to the silyl ether. (c) After 12 h, 92% of acetophenone and all of HSiMe_2Ph have been consumed.

Conclusion

As described above, we confirmed experimentally the difference in reactivity of di-, tri-, and tetra-ruthenium complexes bound to 4,6,8-trimethylazulene toward catalytic hydrosilylation. The triruthenium cluster showed a higher catalytic activity than the other two. Di- and triruthenium clusters, **4** and **3**, were subjected to stoichiometric reactions with PhMe_2SiH , and a disilydiruthenium complex **7** having a Ru–Ru dative bond and a 46-electron silylhydridoruthenium cluster **6** have been isolated and characterized. The diruthenium complex **4** shows low activity in the catalytic hydrosilylation of acetophenone, whereas the disilydiruthenium complex **7** is inactive. This indicates that the formation of **7** from **4** in a potential catalytic cycle hinders the reaction. In contrast, the catalytic activity of the silylruthenium cluster **6** is higher than that of **3**. This provides a possibility that generation of **6** from **3** may

(28) Detailed investigation on the NMR spectrum during the hydrosilylation should give further information on the catalytic intermediates. Unfortunately, attempted assignment of the spectrum shown in Figure 4b was hampered because the existence of dual metallic species, the starting materials, and the products made the NMR spectrum complicated.

be involved in the catalytic hydrosilylation reactions catalyzed by **3**. Furthermore, ^1H NMR measurements in the hydrosilylation of acetophenone with PhMe_2SiH in the presence of a catalytic amount of **6** revealed that **6**, the concentration of which decreased during the course of the reaction, is regenerated after the reactants have been consumed. This suggests that cluster fragmentation is not involved in the reaction. The intermediates in the catalytic cycle could be triruthenium structures closely related to **6**. We consider that these results provide new and interesting aspects in considering molecular cluster species as important intermediates in homogeneous catalysis. Further investigation is in progress on the reactions of multiruthenium carbonyl clusters bearing acenaphthylene or azulene ligands, including more detailed experiments on the transient species derived from the reaction of **6** and organosilanes and on the application of **6** and **7** to other catalytic reactions with hydrosilanes.

Experimental Section

General Procedures. All manipulations were carried out under an argon atmosphere using standard Schlenk techniques. Ether, THF, benzene, toluene, heptane, hexane, and benzene- d_6 were distilled from benzophenone ketyl and stored under an argon atmosphere. All of the other reagents were distilled just before use. NMR spectra were taken with a JEOL Lambda 400 or 600 spectrometer. Chemical shifts were recorded in ppm from the internal standard (^1H , ^{13}C : solvent) or the external standard (^{29}Si : tetramethylsilane). Assignments of the NMR signals were performed with the aid of DEPT and 2D techniques. IR spectra were recorded in cm^{-1} on a JASCO FT/IR-550 spectrometer. The ruthenium complexes **1**, **3**, **4**, and **5** were prepared according to the published methods.^{12,20b,29}

Oxidative Addition of HSiMe_2Ph to $(\mu_3, \eta^5: \eta^5\text{-}4,6,8\text{-Trimethylazulene})\text{Ru}_3(\text{CO})_7$ (3**).** To a solution of **3** (100 mg, 0.15 mmol) dissolved in C_6H_6 (30 mL) was added PhMe_2SiH (102 mg, 0.75 mmol). The mixture was heated at 40°C for 16 h. After removal of the solvent in vacuo, column chromatography (silica gel, ϕ 1.5 \times 5 cm at -78°C) of the residue, by eluting with a 5:1 mixture of hexane and CH_2Cl_2 , gave **6** as a red solid (59 mg, 0.076 mmol; 50% yield), mp 134°C (dec). FAB-MS: 781 ($M + 1$). Anal. Calcd for $\text{Ru}_3\text{SiO}_6\text{C}_{27}\text{H}_{28}$: C, 41.58; H, 3.62. Found: C, 41.17; H, 3.68. Spectroscopic data are listed in Table 2.

(29) Churchill, M. R.; Wormald, J. *Inorg. Chem.* **1973**, *12*, 191.

Oxidative Addition of HSiMe₂Ph to (μ_2, η^3 : η^5 -4,6,8-Trimethylazulene)Ru₂(CO)₅ (4). To a solution of **4** (100 mg, 0.20 mmol) dissolved in C₆H₆ (20 mL) was added PhMe₂SiH (136 mg, 1.00 mmol), and the mixture was heated at 60 °C for 18 h. After removal of the solvent in vacuo, column chromatography (silica gel, ϕ 1.5 × 5 cm at -78 °C) of the residue, by eluting with a 4:1 mixture of hexane and CH₂Cl₂, gave **7** as a yellow solid (90 mg, 0.12 mmol; 60% yield), mp 196 °C (dec). Anal. Calcd for Ru₂Si₂O₄C₃₃H₃₈: C, 52.29; H, 5.06. Found: C, 51.57; H, 4.97. Spectroscopic data are listed in Table 2.

Catalytic Hydrosilylation of Acetophenone. In a 5 mm ϕ NMR tube, acetophenone (0.77 mmol), a trialkylsilane [HSiMe₂Ph or {HSiMe₂(CH₂)₂}] (0.77 mmol), and a catalytic amount of **1**, **3**, **4**, **5**, **6**, or **7** (1 mol %, 7.7 μ mol) were dissolved in C₆D₆ (0.6 mL) containing 1,2-dichloroethane (0.077 mmol). The NMR sample was carefully degassed several times and sealed in vacuo, and ¹H NMR spectra were taken periodically. Identification of the products was performed according to the literature.¹¹ The yield of the products was determined by ¹H NMR, based on the integral value of the internal standard (1,2-dichloroethane).

X-ray Data Collection and Reduction. Crystal data and measurement data of both **6** and **7** are summarized in Table 3. Single crystals of **6** and **7** were grown from a dichloromethane/hexane solution at -30 °C. Data were collected using a Rigaku RAXIS RAPID imaging plate diffractometer with graphite-monochromated Mo K α radiation (λ = 0.71069 Å). All data of **6** and **7** were taken at 296(2) K. Data collection was carried out using the program system MSC/AFC Diffrac-

tometer Control on a Pentium computer. The absorption collection was carried out empirically. The structures were solved by the Patterson method (DIRDIF94 PATTY)^{30a} and were refined using full-matrix least squares (SHELXL97)^{30b} based on F^2 of all independent reflections measured. All non-hydrogen atoms were refined with anisotropic displacement parameters. All H atoms were located at ideal positions and were included in the refinement, but were restricted to ride on the atom to which they were bonded. Isotopic thermal factors of H atoms were held to 1.2–1.5 times (for methyl groups) U_{eq} of the parent atoms.

Acknowledgment. A part of this study was financially supported by the Japan Society for the Promotion of Science (Grants-In-Aid for Scientific Research, 12750768 and 13450374).

Supporting Information Available: The ¹H NOE, ¹H–¹H COSY, ¹H–¹³C HMQC, and ¹H–¹³C HMBC NMR spectra of **6** and **7**, ²D NMR spectra of **6-d_{2.5}** and **7-d₂**, and detailed crystallographic data (excluding structure factors) of **6** and **7** are available free of charge via the Internet at <http://pubs.acs.org>.

OM0200050

(30) (a) Beurskens, P. T.; Admiraal, G.; Beurskens, G.; Bosman, W. P.; de Gelder, R.; Israel, R.; Smits, J. M. M. The DIRDIF-94 program system, Technical Report of the Crystallography Laboratory; University of Nijmegen: The Netherlands, 1994. (b) Sheldrick, G. M. SHELXL-97; 1997.